

Article

Effect of Friction Stir Processing at High Rotational Speed on Aging of a HPDC Mg₉Al₁Zn

Emanuela Cerri *  and Emanuele Ghio 

Department of Engineering and Architecture, University of Parma, 43124 Parma, Italy; emanuele.ghio@unipr.it

* Correspondence: emanuela.cerri@unipr.it; Tel.: +39-0521-905882

Received: 28 June 2020; Accepted: 24 July 2020; Published: 28 July 2020



Abstract: Friction stir processing (FSP) has confirmed its valuable contribution to refining microstructures and the improvement of mechanical properties for Mg-Al alloys. Reference papers illustrate that post-processing aging treatments enhance hardness, but with the application of a solution heat treatment prior to FSP. In this work, aging was performed at two different temperatures (170 and 300 °C) directly on friction stir processed samples of AZ91 produced using high pressure die casting (HPDC). High rotational speeds of the tools (2500 and 3000 rpm) increases the heat input and the temperature of the plates during the process up to 270 °C. Vickers microhardness (HV) increased by 15–20% in the nugget, compared to the as FSPed condition; moreover, a greater homogeneity of hardness values was found at the higher aging temperature used. The β -Mg₁₇Al₁₂ precipitates are randomly distributed inside grains of the stirred area, while in the thermomechanical affected zone (TMAZ) they have grown in a network similar to the old eutectic. A preliminary investigation of FSPed samples deformed at 300 °C found that an equivalent hardness increase is achievable using hot deformation due to dynamic precipitation; to find local homogeneity in hardness, it is worth performing a final aging.

Keywords: FSP; HPDC AZ91; post-process aging; no solution treatment

1. Introduction

Over the past few decades, papers have been published about the application of friction stir processing (FSP) to Mg-Al alloys with the aim of increasing their mechanical properties with emphasis on ductility [1–6]. FSP is a technology that refines the grain size and partially dissolves and breaks up the intermetallic and secondary phases that, in cast Mg-Al alloys, are crucial for defining the final properties. Tensile elongation at room temperature is less than 10%, while significant increase is achieved with a refined grain size [7–12]. Moreover, the break up and partial dissolution of eutectic phases during FSP, due to the increased temperature of the plates, leads to exploiting the idea of artificial aging to obtain an homogeneous reinforcing phase distribution in the stirring zone. The partial dissolution of the eutectic phase and hence the contemporary solute enrichment of the Mg matrix are closely related to the FSP parameters, i.e., the rotational (ω) and advancing speed (V) of the pin, because the temperature of the FSPed plates increases with the ω^2/V ratio. In the context of Mg-Al alloys, AZ91 (Mg–9Al–1Zn) remains one of the most popular ones. It has a good balance of several technological properties such as castability, mechanical strength, corrosion resistance and ductility. Components in AZ91 are now almost all produced using high pressure die casting (HPDC), which ensures better mechanical properties due to the rapid solidification rate. For these reasons, HPDC AZ91 plates have been used for exploiting the effect of high rotational speed FSP on post-aging treatments. Recently, papers were published about the effect of process parameters on aging of Mg alloy such as Mg–Y–Nd [13], Mg–Gd–Y–Zr [14] and Mg–Li [15]. Reference papers for AZ91 are [16,17] where the alloy is solution treated before FSP. In the current experiments, the HPDC

AZ91 is considered for aging after FSP (performed at high speed of rotation) without any previous solution heat treatment, unlike what is found in the literature. The aim of the paper is to study the effect of the friction stir process parameters, especially high speeds of rotation, on post-process aging of the Mg₉Al₁Zn alloy. The microstructure was investigated using optical microscopy (OM), scanning electron microscopy (SEM) and X-ray diffractometry, while the mechanical properties were determined using microhardness measurements.

2. Materials and Methods

Plates 3 mm thick of a HPDC AZ91 magnesium alloy were friction stir processed (FSPed) using a H13 tool steel pin with a truncated cone geometry, having a shoulder diameter of 15 mm and a height of 2.3 mm. Two pin speeds of rotation, ω , (2500 and 3000 rpm) and two advancing speeds, V , (30 and 50 mm/min) were applied as processing conditions. The temperature in the nugget was measured using a K-thermocouple at a distance of 10 mm from the rotating pin. The temperatures were in the range of 220–280 °C, with the highest pertaining to a higher speed of rotation. After FSP, aging was performed at 170 and 300 °C in a muffle furnace for times up to 6 h. Vickers microhardness (HV) and electrical conductivity (EC) were evaluated. HV was measured using a 300 g load for 15 s in the transversal section of the plate. Electrical conductivity was evaluated on the clean surface of the FSPed samples using a FOERSTER-SIGMATEST (FOERSTER, Reutlingen, Germany) device based on the Eddy current principle.

Tensile tests were performed at 300 °C and 10^{-3} s^{-1} to test the effect of aging after hot deformation, with the loading axis normal to the stirring direction.

The microstructure of the FSPed samples was examined using optical microscopy (OM) (Leica DMI8, Wetzlar, Germany) and SEM (ZEISS ULTRA 55, Oberkochen, Germany) at the cross-sectional planes. For OM and SEM observations, samples were mechanically polished to 1 μm with an alcohol-based diamond polishing paste and etched in a solution of 10 mL acetic acid (DASIT GROUP–CARLO ERBA Reagents, Milan, Italy), 4 g picric acid (DASIT GROUP–CARLO ERBA Reagents, Milan, Italy), 50 mL ethanol (DASIT GROUP–CARLO ERBA Reagents, Milan, Italy) and 25 mL distilled water (DASIT GROUP–CARLO ERBA Reagents, Milan, Italy). Grain size was measured using OM on a population of at least 100 grains in the nugget, in the heat affected zone (HAZ) and base material (BM) regions.

Phase identification was also carried out using an X-ray diffractometer using a Cu_α radiation tube working at 30 mA and 40 kV with a measure step of 0.05° for 20 s.

3. Results and Discussion

Figure 1 is an optical micrograph of the sample FSPed at ω of 2500 rpm and V of 30 mm/min showing the cross section of the stirred zone with no visible defects. The BM of the HPDC AZ91 alloy is characterized by a grain size of 8–9 μm (Figure 2a) and by a microstructure typical of the AZ91 HPDC alloy. Figure 2a illustrates its morphology: α -primary (solid solution of Mg) surrounded by the eutectic consisting of α -secondary solid solution and β -phase ($\text{Mg}_{17}\text{Al}_{12}$). Other intermetallics were detected in the HPDC sample, such as AlMn type (Al_6Mn) and MgZn-based phases (Mg_2Zn_3) other than $\text{Mg}_{17}\text{Al}_{12}$ [18]. Figure 2b illustrates the microstructure after FSP (central and upper nugget zones). The coarse intermetallic eutectic network (α -Mg and $\text{Mg}_{17}\text{Al}_{12}$ mainly), typical of the as cast, appears refined after the FSP, and according to the chemical etchant used, it is dark in the picture. It fractured and/or partially dissolved during the process; the Al solute content increased in the matrix, as resulted in [19].

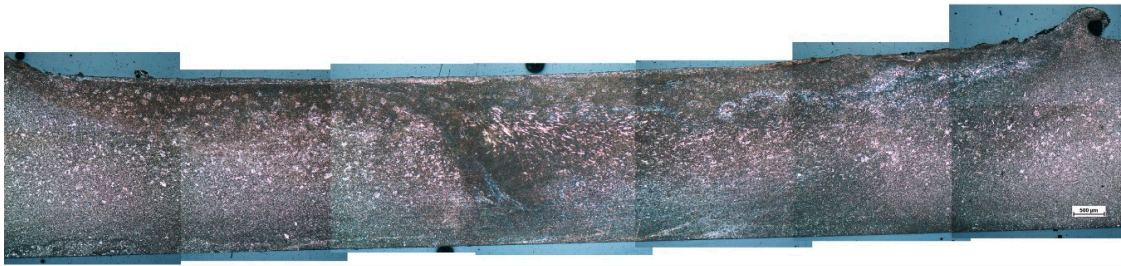


Figure 1. Transversal section of high pressure die casting (HPDC) of AZ91 plate after friction stir processing (FSP) at 2500 rpm and 30 mm/min, showing the nugget zone (the marker length is 500 μm).

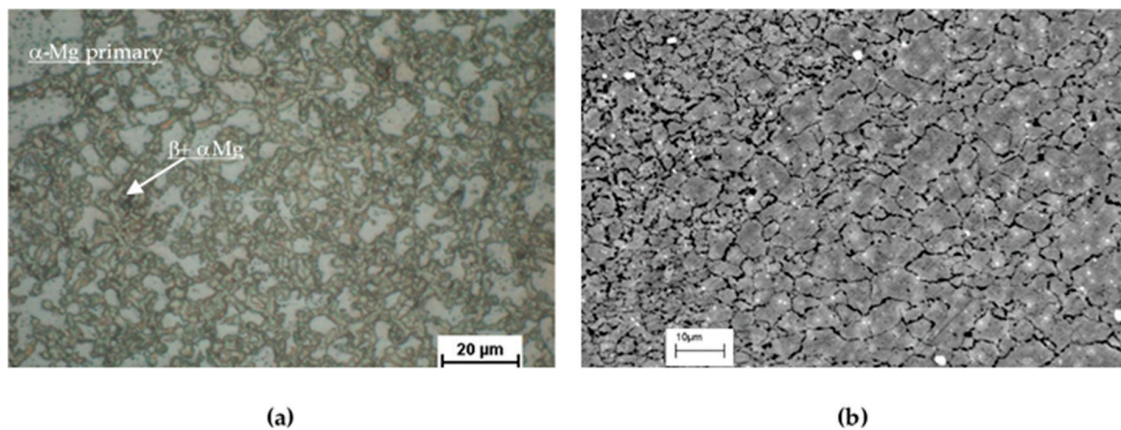


Figure 2. Microstructure of AZ91 magnesium alloy: (a) in the HPDC state (or base material, BM), showing the α -Mg primary and the morphology of the eutectic with the α -Mg secondary and β -phase; (b) after FSP at 2500 rpm and 30 mm/min, illustrating the refinement.

The HV microhardness measurements, performed at the centre of the section perpendicular to the stirring direction, are shown in Figure 3a for samples FSPed at 2500 rpm as a function of the distance from the nugget centre. The HV profiles slightly decline in the stirred area compared to the closest regions, mainly due to the volume reduction of the hard eutectic network during FSP, as shown in Figure 2b. The partial dissolution of the eutectic phases [20] in the stirred area has determined a decrease of electrical conductivity (EC) values in the same region (Figure 3a) and correspondingly the increase of solute atom concentration in the nugget. Out of the stirred zone, the electrical conductivity attains the same values in the retreating and advancing sides of the plate. The EC is lower at the lowest advancing speed (at 30 mm/min) due to the higher heat input developed during FSP (proportional to ω^2/v) and hence to the stronger effectiveness in dissolving the eutectic phases and enriching the α -Mg solid solution. In light of these results obtained for the EC, the FSPed samples were aged at 170 $^{\circ}\text{C}$ to take advantage of the solute in solid solution and hence to increase the hardness. The results are shown in Figure 3b for all the processed samples. Each HV point represents the average value of the Vickers microhardness of the nugget zone (\pm standard deviation). HV remains almost constant in the first two hours and then increases by 10–15% within the next four hours, reaching values between 75–78 HV. The different friction stir process parameters have a slight influence on the aging kinetics at 170 $^{\circ}\text{C}$.

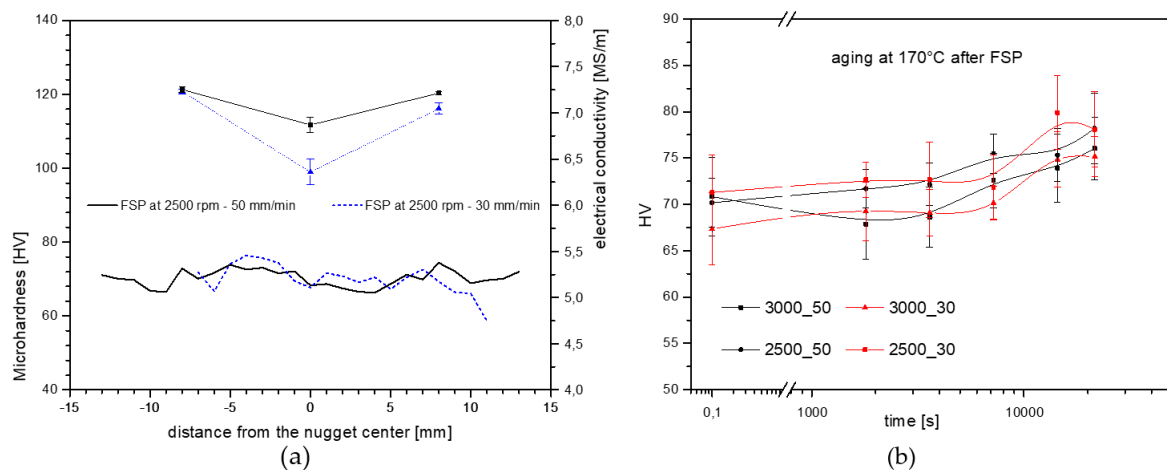


Figure 3. (a) Microhardness profiles and electrical conductivity values for two samples as FSPed and (b) average microhardness at nugget center during aging at 170 °C for each FSPed condition.

Microstructural investigations of main phase modifications induced using FSP and subsequent aging at 170 °C were performed using X-ray diffractometry. Figure 4 illustrates the X-ray diffraction peaks of (330) $Mg_{17}Al_{12}$ and (10–11) α -Mg planes as measured in the BM, after FSP and after subsequent aging at 170 °C for 6 h.

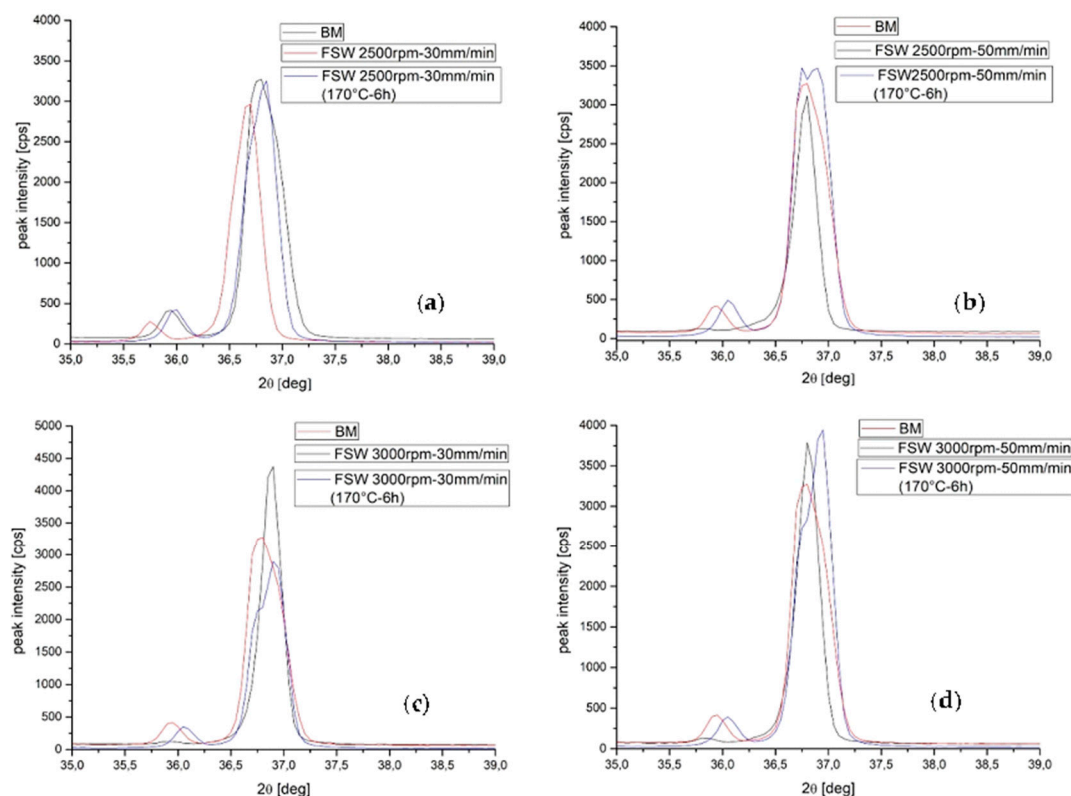


Figure 4. Comparison of X-ray diffractions of FSPed, aged samples at 170 °C-6 h and BM in the four FSP conditions: (a) 2500 rpm, 30 mm/min; (b) 2500 rpm, 50 mm/min; (c) 3000 rpm, 30 mm/min; (d) 3000 rpm, 50 mm/min. The lowest peaks are (330) β - $Mg_{17}Al_{12}$ and the highest are (10–11) Mg.

In the sample FSPed at 2500 rpm-30 mm/min (Figure 4a) the intensity of the β peaks decreases and the α -Mg peaks are shifted to a lower theta angle with respect to reference positions of the BM, i.e., the d_{hkl} spacings increased due to the increased atoms in solid solution. After 6 h aging at 170 °C,

the β phase and the Mg peak return to be similar to the starting condition. In the sample FSPed at 2500 rpm and 50 mm/min (Figure 4b), the β -phase peak disappears after FSP but is present again after 6 h aging, slightly shifted (0.1°) to the right (lower interplanar spacing). In addition, the α -Mg peak is shifted to the right after aging, meaning that interplanar spacing is reduced due to the capture of solute atoms in the precipitated phases (β or $\text{Mg}_{17}\text{Al}_{12}$). X-ray diffraction performed at 3000 rpm (Figure 4c,d) illustrates the same experimental results as for the β -phase and α -Mg. These results confirm the HV curves of Figure 3b, namely that after 6 h aging at 170°C , the hardness is comparable in each sample, independently from the friction stir process condition, as demonstrated using X-ray diffraction.

With the aim of increasing and basically flattening the hardness between the stirred zone and the rest of the plate, FSPed samples were aged at 300°C for times up to 6 h. The microhardness profiles were plotted as a function of distance from the center of the nugget and in the third dimension, reporting the data as a function of time (Figure 5).

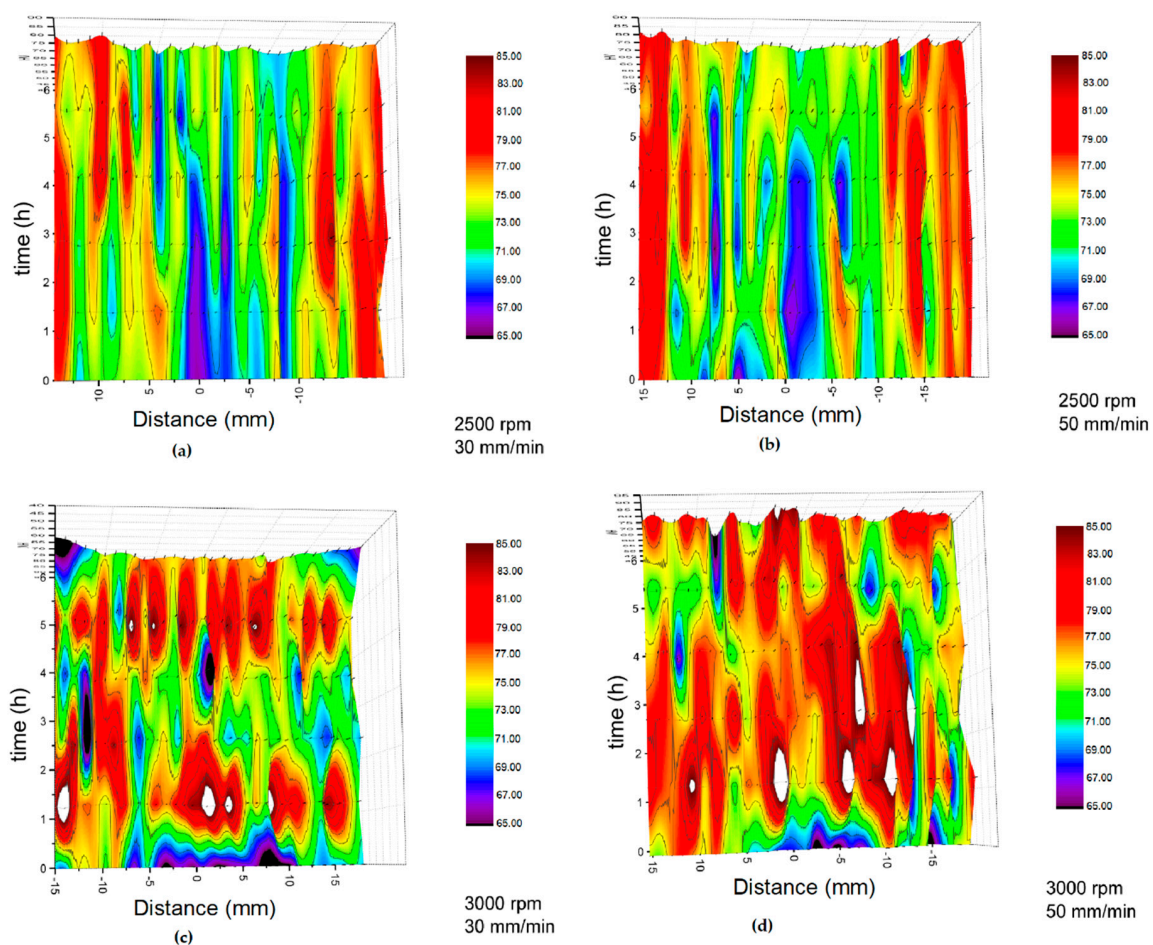


Figure 5. 3D microhardness profiles measured after aging at 300°C in samples FSPed at (a) 2500 rpm, 30 mm/min; (b) 2500 rpm, 50 mm/min; (c) 3000 rpm, 30 mm/min; (d) 3000 rpm, 50 mm/min. Vickers microhardness (HV) profiles are plotted as function of distance from the nugget center (horizontal axis) and at different times (h). The color bands represent HV levels. White regions have hardness > 85 HV.

The aging performed after processing at a lower speed of rotation (Figure 5a,b) shows values < 75 HV in the stirred zones; these values are still lower compared to the rest of the plate (TMAZ (thermo-mechanically affected zone) and HAZ (heat affected zone)). When aging the samples FSPed at 3000 rpm (Figure 5c,d), microhardness values increase in the stirred zones over 80 HV, thus approaching the HV of the rest of the plate. In the sample processed at $v = 50$ mm/min, microhardness exceeds

85 HV (white regions). Ultimately, samples FSPed at 3000 rpm-50 mm/min and aged at 300 °C attain a hardness increase by 15–20% compared to the as FSPed condition.

The microstructure after aging at 300 °C is shown in Figure 6 for the sample FSPed at 2500 rpm-30 mm/min. Light microscopy of the BM zone after aging is shown in Figure 6a, and no precipitates are resolved inside the grains. At the same magnification, when moving towards the TMAZ (Figure 6b), precipitated phases (mainly β -Mg₁₇Al₁₂) are visible like a network surrounding the remaining α -grains. In the nugget area (Figure 6c), the precipitates have entirely grown inside α -Mg grains, as confirmed by the fact that their orientation changes from one grain to another. Figure 6d is a low magnification picture showing the marked border between the nugget and the TMAZ in this magnesium alloy. Figure 6e,f are low and high magnification SEM pictures of the nugget, showing precipitates grown inside the α -Mg matrix.

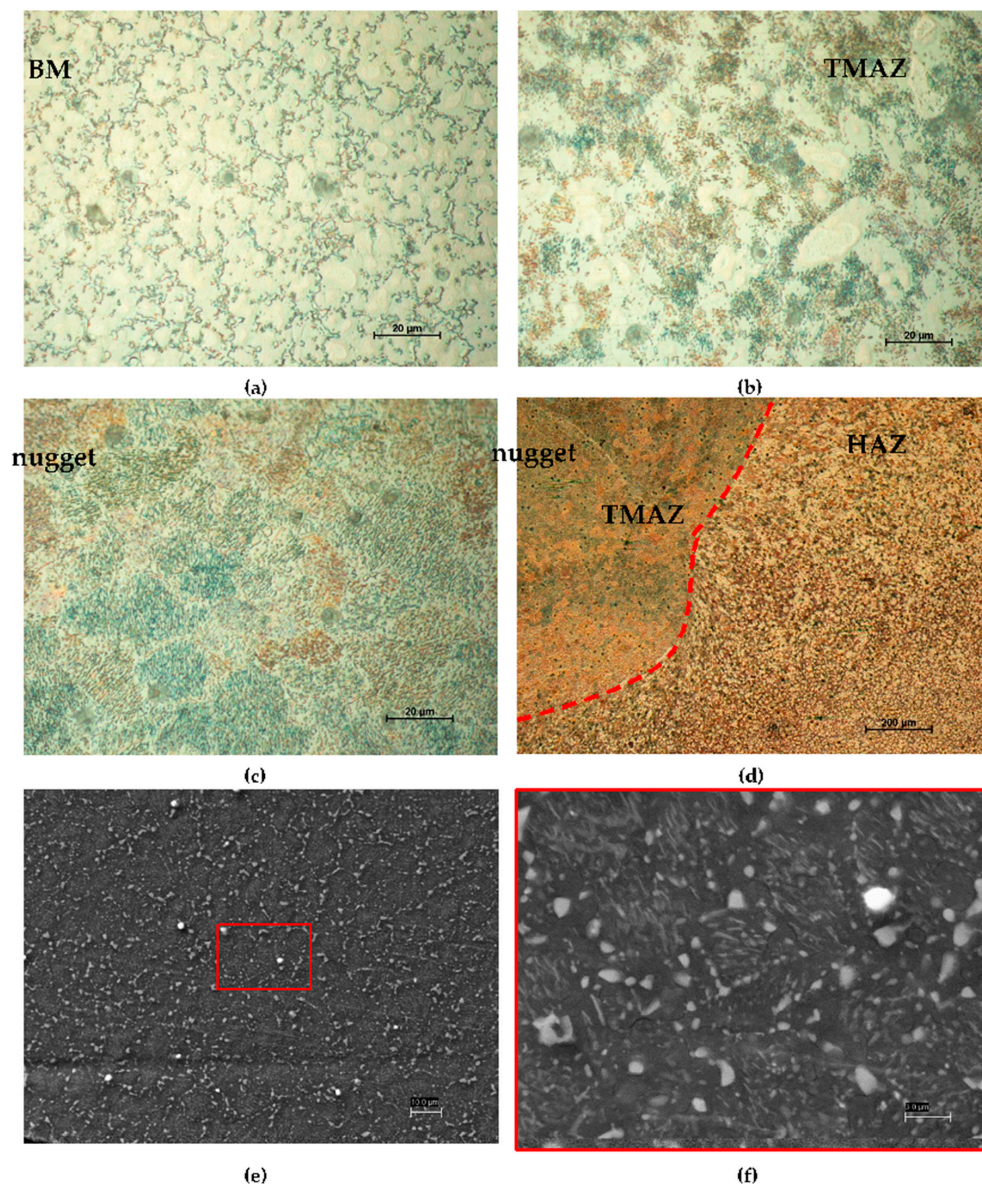


Figure 6. Microstructure of the sample FSPed at 2500 rpm-30 mm/min and aged at 300 °C for 6 h showing precipitate distributions in the characteristic zones. Optical microscopy of (a) base material (BM) zone, (b) thermomechanical affected zones (TMAZ), (c) nugget area and (d) lower magnification picture showing the narrow thermomechanical affected zone (TMAZ) separating the nugget and the HAZ. SEM pictures of the nugget at low (e) and high magnification (f) showing precipitates.

A preliminary investigation on FSPed samples deformed at 300 °C found that an equivalent hardness increase is achievable using hot deformation due to dynamic precipitation; Figure 7 illustrates the hardness measured after aging at 300 °C in the stirring zone (nugget) and in the BM (far from the nugget) of a tensile sample after deformation at 300 °C, for different times up to 6 h. The straining during hot deformation positively contributes to the hardening of the sample after aging, as HV is higher for the nugget compared to the BM area.

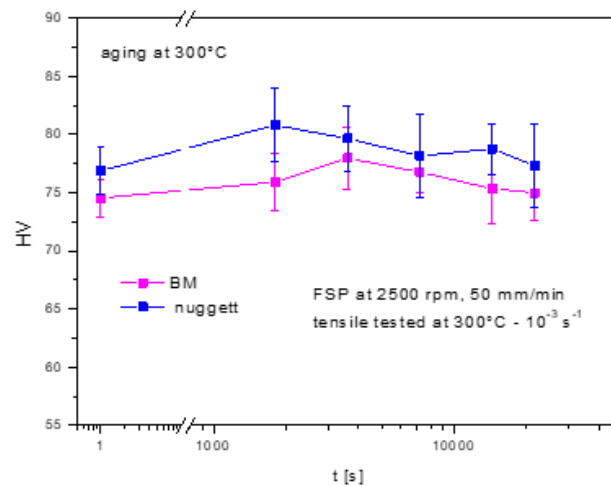


Figure 7. Microhardness measured in the nugget and in the BM regions of tensile samples tested at 300 °C, 10^{-3} s^{-1} and subsequently aged at 300 °C.

4. Conclusions

Aging performed at 170 and 300 °C on an FSPed sample of a HPDC AZ91 magnesium alloy processed at 2500 and 3000 rpm and 30 and 50 mm/min leads to the following conclusions:

1. The process parameters have a slight influence on aging at 170 °C since the hardness values show a small increase with time and the curve for the single process condition varies by 5–6 HV points.
2. The process parameters have more effect on aging at 300 °C, by differentiating the response of the four samples during aging. In this case, there is a similar hardness between the nugget and the remaining zone of the plate. The precipitation is homogeneously distributed in the matrix of the nugget, and it is present in a eutectic shaped area in the TMAZ.
3. The effect of static aging after FSP is comparable to the effect of dynamic aging obtained during hot deformation at 300 °C.

Author Contributions: Conceptualization, methodology, E.C.; software, E.G.; validation, formal analysis, E.C.; investigation, E.G; resources, E.C.; data curation, E.G.; writing—original draft preparation, E.C.; writing—review and editing, E.C., E.G.; visualization, E.C., E.G.; supervision, project administration, funding acquisition, E.C. All authors have read and agreed to the published version of the manuscript.

Funding: This research received no external funding.

Acknowledgments: Authors wish to thank University of Parma for providing the facilities.

Conflicts of Interest: The authors declare no conflict of interest.

References

1. Jain, V.; Su, J.Q.; Mishra, R.S.; Verma, R.; Javaid, A.; Aljarrah, M.; Essadiqi, E. Effect of heat index on microstructure and mechanical behaviour of friction stir processed AZ31. In *Magnesium Technology 2011*; Sillekens, W., Agnew, S., Neelameggham, N., Mathaudhu, S., Eds.; Springer: Cham, Germany, 2011; pp. 205–209.

2. Chang, C.I.; Du, X.H.; Huang, J.C. Achieving ultrafine grain size in Mg-Al-Zn alloy by friction processing. *Scr. Mater.* **2007**, *57*, 209–212. [[CrossRef](#)]
3. Park, S.H.C.; Sato, S.Y.; Kokawa, H. Basal plane texture and flow pattern in friction stir weld of a magnesium alloy. *Metal. Mater. Trans. A* **2003**, *34*, 987–994. [[CrossRef](#)]
4. Yuan, W.; Mishra, R.S. Grain size and texture effects on deformation behaviour of AZ31 magnesium alloy. *Mater. Sci. Eng. A* **2012**, *558*, 716–724. [[CrossRef](#)]
5. Yu, Z.; Choo, H.; Feng, Z.; Vogel, S.C. Influence of thermo-mechanical parameters on texture and tensile behaviour of friction stir processed Mg alloy. *Scr. Mater.* **2010**, *63*, 1112–1115. [[CrossRef](#)]
6. Chang, C.I.; Lee, C.J.; Huang, J.C. Relationship between grain size and Zener-Holloman parameter during friction stir processing in AZ31 Mg alloys. *Scr. Mater.* **2004**, *51*, 509–514. [[CrossRef](#)]
7. Watanabe, H.; Mukai, T.; Ishikawa, K.; Mabuchi, M.; Higashi, K. Realization of high-strain-rate superplasticity at low temperature in a Mg-Zn-Zr alloy. *Mater. Sci. Eng. A* **2001**, *307*, 119–128. [[CrossRef](#)]
8. Mohan, A.; Yuan, W.; Mishra, R.S. High strain rate superplasticity in friction stir processed ultrafine grained Mg-Al-Zn alloys. *Mater. Sci. Eng. A* **2013**, *562*, 69–76. [[CrossRef](#)]
9. Jain, V.; Mishra, R.S.; Gouthama. Superplastic behaviour and microstructural stability of friction stir processed AZ91C alloy. *J. Mater. Sci.* **2013**, *48*, 2635–2646. [[CrossRef](#)]
10. Chai, F.; Zhang, D.; Li, Y.; Zhang, W. High strain rate superplasticity of a fine-grained AZ91 magnesium alloy prepared by submerged friction stir processing. *Mater. Sci. Eng. A* **2013**, *568*, 40–48.
11. Del Valle, J.A.; Rey, P.; Gestó, D.; Verdura, D.; Jiménez, J.A.; Ruano, O.A. Mechanical properties of ultra-fine grained AZ91 magnesium alloy processed by friction stir processing. *Mater. Sci. Eng. A* **2015**, *628*, 198–206.
12. Feng, A.H.; Ma, Z.Y. Enhanced mechanical properties of Mg-Al-Zn cast alloy via friction stir processing. *Scr. Mater.* **2007**, *56*, 397–400. [[CrossRef](#)]
13. Cao, G.H.; Zhang, D.T.; Luo, X.C.; Zhang, W.W.; Zhang, W. Effect of aging treatment on mechanical properties and fracture behaviour of friction stir processed Mg-Y-Nd alloy. *J. Mater. Sci.* **2016**, *51*, 7571–7584. [[CrossRef](#)]
14. Xiao, B.; Yang, D.; Yang, J.; Wang, W.G.; Xie, G.M.; Ma, Z.Y. Enhanced mechanical properties of Mg-Gd-Y-Zr casting via friction stir processing. *J. Alloy. Compd.* **2011**, *509*, 2879–2884. [[CrossRef](#)]
15. Yang, C.W.; Chen, Y.W. Effects of artificial aging and precipitation on tensile mechanical properties and failure mechanism of the friction stir processed Dual-phase Mg-Li alloy. In Proceedings of the 7th International Conference on Materials for Advanced Technologies (ICMAT2013), Singapore, 30 June–13 July 2013.
16. Jain, V.; Mishra, R.S.; Gupta, A.K.; Gouthama. Study of beta-precipitates and their effect on the directional yield asymmetry of friction stir processed and aged AZ91C alloy. *Mater. Sci. Eng. A* **2013**, *560*, 500–509. [[CrossRef](#)]
17. Feng, A.H.; Ma, Z.Y. Microstructural evolution of cast Mg-Al-Zn during friction stir processing and subsequent aging. *Acta Mater.* **2009**, *57*, 4248–4260. [[CrossRef](#)]
18. Cerri, E.; Leo, P.; De Marco, P. Hot compression behaviour of the AZ91 magnesium alloy produced by high pressure die casting. *J. Mater. Proc. Technol.* **2007**, *189*, 97–106. [[CrossRef](#)]
19. Cerri, E.; Cabibbo, M.; Leo, P. Nanoindentation and microstructure of Friction Stir Processed Die Cast Mg-Al-Zn alloy. *Met. Ita.* **2014**, *5*, 3–10.
20. Cerri, E.; Renna, G.; Cabibbo, M.; Simoncini, M.; Forcellese, A. Friction stir processing at high rotation rates of a magnesium alloy: Mechanical properties at high temperatures and microstructure. *Mater. Sci. Forum* **2017**, *879*, 295–300. [[CrossRef](#)]

